Biol. Cybernetics 28, 143—157 (1978)

Biological Cybernetics

A General Myocybernetic Control Model of Skeletal Muscle

H. Hatze

National Research Institute for Mathematical Sciences, CSIR, Pretoria, South Africa

Abstract. A general myocybernetic control model of skeletal muscle is presented which constitutes an extension, to general control modes, of a previously published control model. The restriction, in the previous model, to a constant number of stimulated motor units has been removed and the new model allows for both a varying number of stimulated motor units and a varying average stimulation rate. The general model is tested by comparing its predictions with experimental records of the force output of the quadriceps femoris muscle. It is found that the model correctly predicts the initial excitation-contraction delay, the dips in the force record, and several other contraction phenomena.

Introduction

In (Hatze, 1977a) a detailed representation was given of a myocybernetic model of skeletal muscle, i.e. of a mathematical muscle model which contains the physiological controls stimulation rate and motor unit recruitment as explicit parameters. It was shown that this model is capable of predicting a wide variety of experimentally established phenomena of muscular contraction. Moreover, a simplified version was successfully used in the optimization of a human motion.

It is interesting to note that increasingly more experimental evidence is accumulating in support of previously unconfirmed predictions or assumptions of the model: Edman et al. (1976) have recently demonstrated that the force-velocity relation of single fibres as well as bundles of fibres of the frog cannot be fitted satisfactorily by Hill's equation, a fact predicted by the present model. On the other hand, the force-velocity function as obtained by these workers can be approximated very closely by the corresponding function of the present model. In another recent report, Briggs et al. (1977) have concluded on the grounds of experimental evidence that the ratio of the rates of uptake of Ca^{2+} by the sarcoplasmic reticulum for fast and slow mammalian (rat, cat) muscles is about five. The present model [upper part of Figure 3 of Hatze (1977a)] predicts, on purely theoretical grounds, a corresponding value of about four for human muscle.

Reassuring as these experimental confirmations of the model structure may be, there remains a disturbing fact about the model: although it is completely general in its contraction dynamics, one of its control parameters (the relative number u of active fibres) is restricted to constant values. This is an obvious consequence of the constancy constraint imposed by Equation (42) of Hatze (1977a) on the number ϱ of stimulated muscle fibres. [Note that the simplified version of the model [Equation (53) of Hatze (1977a)] requires the control $u(t)$ to be only *piecewise* constant for arbitrarily small time intervals Δt, since in this version $\varrho(t)$ is no longer required to remain constant throughout the whole simulation interval.]

Although the restricted model has its merits, for example in the prediction of energy-optimal controls and the relative contribution of motor unit recruitment and rate coding in static isometric contractions (Hatze and Buys, 1977; Hatze, 1977b), it is nevertheless inappropriate for simulating contractive modes where *both* controls, the stimulation rates of the activated motor units and the number of stimulated units, vary as functions of time. But this is exactly the mode most frequently occurring in the living biosystem and it is, therefore, of paramount importance.

This paper will be devoted to the development of a general myocybernetic model which accounts for all control modes normally occurring in living muscle, and which will be seen to provide good approximations to the responses of the distributed system, consisting of individual motor units, for the most extreme test control modes.

0340-1200/78/0028/0143/$03.00

Derivation of the General Model

Most of the more intricate mathematical treatment will be transferred to the Appendix in order not to distract the reader from the main development.

We shall set out from the differential system which described the previous model (for details see Hatze, 1977a), i.e.

$$\begin{aligned}
&\dot{\gamma}=m(cv-\gamma), && \gamma(0)=0,\\
&\dot{\varepsilon}=m\mu(cv-\gamma), && \varepsilon(0)=q_0,\\
&\dot{\mu}=m(cv-\gamma)\varrho_1(\xi)[\varrho_1(\xi)\{u(1-q_0)+q_0-\varepsilon\}-2\varrho_2\mu], && \mu(0)=0,\\
&\dot{\xi}=(-\dot{\bar{\lambda}}_0/\bar{\lambda})\left[a_2+a_1^{-1}\operatorname{arctanh}\left\{\frac{[F^{SE}(l,\xi)/\bar{F}\sin\theta(\xi)+b_1\exp(-a_6(\xi-1))]b_2}{\varepsilon k(\xi)}-1\right\}\right], && \xi(0)=\xi_0,
\end{aligned} \tag{1}$$

where the first three equations define the *excitation dynamics* and the last equation defines the *contraction dynamics* of the model. The symbols have the following meaning: γ denotes the free ionic Ca-concentration in the sarcoplasma of an "average" fibre, ε is the excitation variable, μ is an auxiliary variable, ξ is the relative length of the contractile element of the muscle, and u (the relative number of active fibres) and v (the relative average stimulation rate) are the two control parameters of the muscle and subject to the constraints

$$0\leqq u,v\leqq 1\,. \tag{2}$$

Furthermore, the symbols m, c, q_0, ξ_0, ϱ_2, a_1, a_2, a_6, b_1, b_2, $\bar{\lambda}$, $\bar{F}$ (maximum force produced by contractile element), and $\dot{\bar{\lambda}}_0$ denote muscle-specific constants (exactly defined in Hatze, 1977a), while $k(\xi)$ is the length-tension relation, and the function $\varrho_1(\xi)$ is given by (Hatze, 1977a)

$$\begin{aligned}
&\varrho_1(\xi)=\bar{r}[1-(\check{\xi}/\xi)^s]^{1/2}/[1-\check{\xi}^s]^{1/2},\\
&\qquad \check{\xi}\leqq\xi\leqq 1.8\,,
\end{aligned} \tag{3}$$

$\bar{r}$, $\check{\xi}$, and s being constants. The function $\sin\theta(\xi)$ appearing in (1) is defined by $\sin\theta(\xi)\equiv 1$ for *fusiform muscles* (fibres arranged in longitudinal direction), and by $\sin\theta(\xi)=\left[1-\left(\frac{\bar{l}_f\cos\bar{\theta}}{\bar{\lambda}(\xi-1)+\bar{l}_f}\right)^2\right]^{1/2}$ for *penniform muscles* [oblique fibre arrangement; Hatze (1976)], where $\bar{l}_f$ and $\bar{\theta}$ denote constants defined below. The force across the series elastic element of the muscle is given by

$$F^{SE}(l,\xi)=\bar{F}\sin\bar{\theta}[\exp(\sigma\delta)-1]/[\exp(\sigma)-1]\,, \tag{4}$$

where for *fusiform muscles* $\bar{\theta}\equiv\frac{1}{2}\pi$, and

$$\delta=(l+\bar{\lambda}(1-\xi)-(1-\bar{\zeta})\bar{l})/\bar{\zeta}\bar{l}\,, \tag{5}$$

with l denoting the muscle length (including the series elastic element), and σ, $\bar{\zeta}$, $\bar{l}$ are again muscle-specific constants. For *penniform muscles* the expression

$$\bar{l}_f\sin\bar{\theta}-[\{\bar{\lambda}(\xi-1)+\bar{l}_f\}^2-\{\bar{l}_f\cos\bar{\theta}\}^2]^{1/2}$$

must be substituted for $\bar{\lambda}(1-\xi)$ in (5), where $\bar{\theta}$ is the angle of inclination of the fibre to the perpendicular to the muscle's long axis when $l=\bar{l}$, and $\bar{l}_f$ is the fibre length when $l=\bar{l}$.

The differential equation defining the excitation variable ε in (1) was derived from the definition

$$\begin{aligned}
\varepsilon&\triangleq(1/\bar{\varrho})\left[\sum_{i=1}^{\varrho}q_i(\xi,v_i,t)+\sum_{j=\varrho+1}^{\bar{\varrho}}q_{0j}\right]\\
&\triangleq u[q(\xi,v,t)-q_0]+q_0\,,
\end{aligned} \tag{6}$$

where $u\triangleq(\varrho/\bar{\varrho})$, and the "average active state" $q(\xi,v,t)$ was defined by a certain differential equation. The restricting assumption was that the number ϱ of stimulated muscle fibres having an average active state $q(\cdot)$ remains constant; which, in turn, implies a constant value of the control u. Indeed, this constancy requirement makes it possible to eliminate the second and third equations from the differential system (1). By introducing the variable transformation

$$\omega\triangleq\varrho_1(\xi)\gamma,\quad \varrho_1(\xi)\neq 0\,, \tag{7}$$

it is easily shown that the analytical solution of these two coupled equations is given by

$$\begin{aligned}
\varepsilon(u,\omega)=u(1-q_0)[1-(&m_1\exp(m_2\omega)\\
&-m_2\exp(m_1\omega))/(m_1-m_2)]+q_0\,,
\end{aligned} \tag{8}$$

where (see Hatze, 1977a)

$$m_{1,2}=-\varrho_2\pm(\varrho_2^2-1)^{1/2},\quad \varrho_2=1.05\,.$$

Hence ε as a *state* can be eliminated from (1) and now becomes the excitation *function*. Re-substituting from (7) and putting $u\equiv 1$ in (8) we obtain the following expression for the active state $q(\xi,\gamma)$ of a single fibre:

$$\begin{aligned}
q(\xi,\gamma)=1-(1-q_0)[&m_1\exp(m_2\varrho_1(\xi)\gamma)\\
&-m_2\exp(m_1\varrho_1(\xi)\gamma)]/(m_1-m_2)\,,
\end{aligned} \tag{9}$$

which is the relation needed for the further development.

We shall now derive the general model from first principles. Because we are now dealing with a *varying* number of stimulated *motor units* (in contrast with a *fixed* number of stimulated *fibres* in the previous model), the specific properties of the former must be taken into account.

By now it has been fairly well documented (Desmedt and Godaux, 1977; Grimby and Hannerz, 1977; Henneman, 1968; Henneman et al., 1965; Milner-Brown et al., 1973; etc.) that motor units are recruited in a sequential order, according to their sizes, in all types of contractions (static isometric, isometric ramp, reflex, brisk ballistic) and that the cumulative relative cross-sectional area u occupied by the fibres of the recruited units increases according to (Hatze, 1977c; Hatze and Buys, 1977)

$$u = u_0 \exp(N\bar{c}/\bar{N}), \quad 0 < u_0 \leqq u \leqq 1 , \tag{10}$$

where the constant $\bar{c}$ has a value of about five for most muscles and is related to u_0 by $\bar{c} = -\ln u_0$; N denotes the number of stimulated motor units; and $\bar{N}$ is the total number of units present in a specific muscle. Note that u has here the same meaning as in (1).

The infinitesimal increment $\Delta_i u$ of the relative cross-sectional area u upon recruitment of the i-th unit follows from (10) as

$$\Delta_i u = A \exp(\bar{c}i/\bar{N}) , \tag{11}$$

where the constant A is determined by the requirement

$$\sum_{i=1}^{\bar{N}} \Delta_i u = 1, \text{ i.e.}$$

$$A = 1 \Big/ \sum_{i=1}^{\bar{N}} \exp(\bar{c}i/\bar{N}) .$$

In (Hatze, 1977a) it has been shown that the force F^{CE} produced by the contractile element of the total muscle comprising $\bar{\varrho}$ fibres can be expressed as

$$F^{CE} = \sum_{i=1}^{\bar{\varrho}} f_i^{CE} = \sum_{i=1}^{\bar{\varrho}} \bar{f}_i [k(\xi) q_i(\xi, v_i, t) h_i(\dot{\xi}) - b_{1i} k_1(\xi)] ,$$

where $\bar{f}_i$ is the maximum tetanic force of the i-th fibre,

$$h_i(\dot{\xi}) = [1 + \tanh\{a_{1i}(-\dot{\xi}\bar{\lambda}/\dot{\bar{\lambda}}_{0i} - a_{2i})\}]/b_{2i} ,$$

$$k_1(\xi) = \exp[-a_6(\xi - 1)] ,$$

and all other symbols have the meanings defined previously. In the present case we are dealing with a total of $\bar{N}$ motor units (instead of $\bar{\varrho}$ fibres), N of which are stimulated, R unstimulated but still active (semi-active), and $(\bar{N} - N - R)$ inactive. Since $\bar{f}_i = \bar{F}\Delta_i u$, the expression for the force output then becomes

$$F^{CE} = \bar{F}\Big[k(\xi)\Big\{\sum_{i=1}^{N(t)} \Delta_i u q_i(\xi, \gamma_i^+) h_i(\dot{\xi}) + \sum_{j=N(t)+1}^{N(t)+R(t)} \Delta_j u q_j(\xi, \gamma^-) h_j(\dot{\xi}) + q_0 \sum_{k=N(t)+R(t)}^{\bar{N}} \Delta_k u h_k(\dot{\xi})\Big\} - k_1(\xi) \sum_{i=1}^{\bar{N}} \Delta_i u b_{1i}\Big], \tag{12}$$

where γ^+ and γ^- denote the Ca-concentrations of the stimulated and semi-active units respectively, and this expression indicates that the total force output of the muscle is composed of the individual forces contributed by each of the $\bar{N}$ motor units. Each of these units belongs to one of three types of dynamic unit populations present in the muscle: the N-population of *stimulated* units, the R-population of units which were stimulated but had been switched off some time ago and are still active (so-called *semi-active* units), and the population of *inactive* (resting) units.

The severe difficulties bedevilling the modelling of the present situation can be appreciated when the following general contractive mode is considered: N units, all of different size and with different contractive properties, were activated at different times t_i by different stimulation rates v_i. Hence the expressions

$$\Delta_i u q_i(\xi, \gamma_i^+(v_i(t - t_i))) h_i(\dot{\xi})$$

in (12) are all different, nonlinear functions of time, delayed in their onset by $(t - t_i)$. If now $N(t)$ increases, the N-population absorbs part of the semi-active R-population, all units of which have different active states since they have been switched on and off at various previous times.

The first step in simplifying this complex situation somewhat is to consider only *parts* of the muscle comprising motor units of (approximately) *homogeneous fibre type*. Then the velocity-dependence function $h(\dot{\xi})$ and the constant b_1 are the same for all units and (12) becomes

$$F^{CE} = \bar{F}k(\xi)h(\dot{\xi})\varepsilon(t) - \bar{F}b_1 k_1(\xi) ,$$

where the *excitation function* ε *for the general model* is now defined by

$$\varepsilon(t) \triangleq \sum_{i=1}^{N(t)} \Delta_i u q_i(\xi, \gamma_i^+(v_i(t - t_i))) + \sum_{j=N(t)+1}^{N(t)+R(t)} \Delta_j u q_j(\xi, \gamma_j^-(t)) + \sum_{k=N(t)+R(t)}^{\bar{N}} \Delta_k u q_0 . \tag{13}$$

Note that (13) is completely analogous to (6) which was derived under similar assumptions.

It is clear that we cannot hope to find a simple model which describes the behaviour of the system *exactly* (otherwise, nature would presumably not have devised such a complex system). However, we shall show that it is possible to derive a model which very *closely approximates* the real system for a wide variety of contractive modes.

Definition (13) can be concisely written as

$$\varepsilon(t)=\varepsilon^{+}(t)+\varepsilon^{-}(t)+\varepsilon^{0}(t)\,, \tag{14}$$

where

$$\varepsilon^{+}(t)\triangleq A\sum_{i=1}^{N(t)}\exp(\bar{c}i/\bar{N})q_i(\xi,\gamma_i^{+}(v_i(t-t_i)))\,, \tag{15}$$

$$\varepsilon^{-}(t)\triangleq A\sum_{j=N(t)+1}^{N(t)+R(t)}\exp(\bar{c}j/\bar{N})q_j(\xi,\gamma_j^{-}(t))\,, \tag{16}$$

$$\varepsilon^{0}(t)\triangleq q_0[\exp(\bar{c})-\exp(\bar{c}(N+R)/\bar{N})]/[\exp(\bar{c})-1]\,, \tag{17}$$

with

$$A\triangleq 1\Big/\sum_{i=1}^{\bar{N}}\exp(\bar{c}i/\bar{N})\,. \tag{18}$$

We shall now show that it is possible to find functions ("equivalent Ca-concentrations") $\psi(\cdot)$ and $\varphi(\cdot)$ such that

$$\varepsilon^{+}(t)\approx Aq(\xi,\psi(\cdot))\sum_{i=1}^{N(t)}\exp(\bar{c}i/\bar{N}) \tag{19}$$

and

$$\varepsilon^{-}(t)\approx Aq(\xi,\varphi(\cdot))\sum_{j=N(t)+1}^{N(t)+R(t)}\exp(\bar{c}j/\bar{N})\,, \tag{20}$$

where $q(\cdot)$ is as given by (9). It will be seen that the differential equations defining the functions $\psi(\cdot)$ and $\varphi(\cdot)$ contain the control v and a new control, z, which will be defined in due course. The previous control u will, however, no longer appear in the system. Note that the procedure indicated by (19) and (20) will enable us to derive a comparatively simple system of equations, the solutions of which will be seen to provide good approximations to the solutions of the exact system, defined by (15)–(17).

The derivation of the differential system which describes the general model is somewhat involved and has therefore been transferred to the Appendix. In short, the fact that $\bar{N}$ is generally very large is used to approximate discrete functions by continuous and piecewise differentiable ones, and sums by integrals. The resultant integral equations are subsequently differentiated, totally with respect to t and partially with respect to other variables, which procedure finally leads to the *state equations for the general model:*

$$\begin{aligned}
&\dot{n}=\hat{n}z\,, \quad 0\leqq n\leqq 1\,, && n(0)=0\,,\\
&\dot{r}=-\hat{n}z(r-w^{-}\bar{\delta})/(r+\bar{\delta})-(1+w^{-})mr/\ln(1+10^{-3}m+\varphi/k_2c)\,, && r(0)=0\,,\\
&\dot{\psi}=m(cv-\psi)+w^{+}z\bar{c}\hat{n}[1-\exp\{\varrho_0(\xi)(\psi-\varphi)\}]/[\varrho_0(\xi)(1-\exp(-\bar{c}n-\bar{\delta}))]-(1+w^{-})\varphi m\,, && \psi(0)=0\,,\\
&\dot{\varphi}=-\varphi m-w^{-}\{m(cv/(\psi+\bar{\delta})-1)\varphi-z\bar{c}\hat{n}[1-\exp\{\varrho_0(\xi)(\varphi-\psi)\}]/[\varrho_0(\xi)(\exp(\bar{c}r+\bar{\delta})-1)]\}\,, && \varphi(0)=0\,,\\
&\dot{\xi}=(-\dot{\lambda}_0/\bar{\lambda})\left[a_2+a_1^{-1}\operatorname{arctanh}\left\{\frac{[F^{\mathrm{SE}}(l,\xi)/\bar{F}\sin\theta(\xi)+b_1\exp(-a_6(\xi-1))]b_2}{\varepsilon k(\xi)}-1\right\}\right], && \xi(0)=\xi_0\,,
\end{aligned} \tag{21}$$

where the initial conditions refer to the resting state of the muscle.

The various symbols (not previously defined) are defined as follows. The *normalized number of stimulated motor units*, n, is given by

$$n\triangleq N/\bar{N}\,, \quad 0\leqq n\leqq 1\,, \tag{22}$$

while the *normalized number of semi-active units*, r, is defined by

$$r\triangleq R/\bar{N}\,, \quad 0\leqq r\leqq 1\,. \tag{23}$$

The symbols $\hat{n}$ (the maximum rate of unit recruitment), $\bar{\delta}$ (with a value of 10^{-8}), and k_2 denote constants. Note that the small constant $\bar{\delta}$ has been added to the respective variables in order to obviate division by zero. It can be shown that this procedure does not significantly influence the accuracy of the solution. The function $\varrho_0(\xi)$ is given by

$$\varrho_0(\xi)=5.33\times 10^4[1-(\check{\xi}/\xi)^s]^{1/2}/[1-\check{\xi}^s]^{1/2}\,, \quad \check{\xi}\leqq\xi\leqq 1.8\,, \tag{24}$$

and w^{+} and w^{-} are defined by the respective relations

$$\begin{aligned} w^{+}&=w(1+w)/2\,,\\ w^{-}&=w(1-w)/2\,, \end{aligned} \tag{25}$$

where the *switching function* (the *switch*) $w=w(z)$ is expressed by

$$w\triangleq\operatorname{sgn}(z)\,, \tag{26}$$

i.e.

$$\begin{aligned} w&=1 \quad \text{for} \quad z>0\,,\\ &=0 \quad \text{for} \quad z=0\,,\\ &=-1 \quad \text{for} \quad z<0\,. \end{aligned}$$

The second control (in addition to v) appearing in (21) is the *normalized recruitment rate*, z, which is subject to the constraints

$$-\check{z}\leqq z\leqq 1\,, \tag{27}$$

$\check{z}$ being a positive constant. The *excitation function* ε which appears in the last of Equations (21) is given by (14) or, more explicitly, by

$$\begin{aligned} \varepsilon=&[(\exp(\bar{c}n)-1)q(\xi,\psi)\\ &+(\exp(\bar{c}n+\bar{c}r)-\exp(\bar{c}n))q(\xi,\varphi)\\ &+(\exp(\bar{c})-\exp(\bar{c}n+\bar{c}r))q_0]/[\exp(\bar{c})-1]\,, \end{aligned} \tag{28}$$

where $q(\cdot)$ is basically the function (9). However, (9) can be closely approximated by the much simpler function

$$q(\xi,\gamma)=[q_0+(\varrho(\xi)\gamma)^2]/[1+(\varrho(\xi)\gamma)^2]\,, \tag{29}$$

with

$$\varrho(\xi)=6.62\times 10^4[1-(\check{\xi}/\xi)^s]^{1/2}/[1-\check{\xi}^s]^{1/2}\,.$$

From now on, the approximation (29) will be used instead of (9).

If we now compare the systems (1) and (21) we see that they are completely analogous, and that the latter system reflects the changes introduced by the inclusion of the recruitment dynamics: the excitation function ε [recall that ε as a state had been removed from (1)] given by (8) has its counterpart in (28), while the average free Ca-concentration γ is replaced by the "pseudo" or "equivalent" Ca-concentrations ψ for the stimulated units, and φ for the semi-active units respectively. The *recruitment dynamics* in the general model is represented by the first two differential equations in (21) which define the states n and r. The control u has been replaced by the state n, and the new control z is now a *rate* (the *normalized recruitment rate*) like the control v (the *normalized firing rate*).

Thus, the first four of Equations (21) represent the *excitation dynamics* of the general model while the *contraction dynamics*, described by the last of Equations (21), is the same as in the model (1).

The general model has several advantages over the previous one. These will be discussed after the model has been validated by simulation and then verified by comparison with experimental results.

Validation of the General Model

The most logical thing to do is obviously to compare the responses of the approximating system (21) with the responses of the exact system, made up of the sum of the individual responses of many separate motor units, just as occurs in the living muscle. The test should be carried out for the most extreme control modes possible. This is precisely the type of simulation we shall now perform. Since the contraction dynamics is the same for all motor units, provided they are all of the same type (fast, intermediate, slow), we have only to compare the excitation functions ε of the approximating and of the exact system.

The function ε for the *exact system* is simply [see (14)–(18)]

$$\varepsilon=A\sum_{i=1}^{\bar{N}}\exp(\bar{c}i/\bar{N})q_i(\xi,\gamma_i)\,, \tag{30}$$

where $q_i(\cdot)$ is given by (29) with γ_i defined by the differential system (for details see Hatze, 1977a):

$$\begin{aligned}&\ddot{\beta}_i+c_4\dot{\beta}_i+c_5\beta_i=c_6V_N\alpha_i(t)\,, \quad \beta_i(0)=\dot{\beta}_i(0)=0\,,\\ &\ddot{\gamma}_i+c_1\dot{\gamma}_i+c_2\gamma_i=c_3V_T\beta_i\,, \quad \gamma_i(0)=\dot{\gamma}_i(0)=0\,,\end{aligned} \tag{31}$$

where

$$\begin{aligned}&\alpha_i(t)=\sin 1000\pi(t-t_j) \quad \text{for} \quad t_j\leqq t\leqq t_j+0.001\,,\\ &\quad=0 \quad \text{otherwise}, \quad j=1,2,\ldots\,.\end{aligned}$$

In Figure 7 of Hatze (1977a) it has been shown that the train $\alpha_i(t)$ of nerve impulses produces a train $q_i(\xi,\gamma_i(t))$ of active state twitches and corresponding force twitches which are precisely (time course, magnitude of peak tension, half-relaxation time, etc.) those obtained in many experiments on living muscle. Hence the output $q_i(\xi,t)$ of the system (29) plus (31) can be regarded as truly representative of the active state of the i-th motor unit, which also means that ε, as given by (30), is representative of the excitation of the real muscle.

The function ε for the *approximating system* is given by (28) with the various variables defined by (21), and with the normalized "average" firing rate v given by

$$v=\left[\sum_{i=1}^{N}v_i\exp(\bar{c}i/\bar{N})\right]\Big/\left[\sum_{i=1}^{N}\exp(\bar{c}i/\bar{N})\right], \tag{32}$$

where $v_i=1/\hat{v}\tau_i$ is the normalized firing rate of the i-th motor unit, $\hat{v}$ denoting the maximum firing rate.

It was decided to perform the simulation for *fast* motor units because their fast responses permit the simulation of more effects in a given time interval. We shall use the same constants for fast muscle as those described in Hatze (1977a, Table 1), except for the constants c_3, c, and $\bar{r}$ which were adjusted to account for more accurate results (Briggs et al., 1977; Ebashi and Endo, 1968) on the magnitude of the free Ca ion concentration γ in the sarcoplasm during stimulation [our previous values had been taken from Julian (1971)]. Note that this change in the values of the constants involves only a scaling transformation ($\gamma_{\max}$ has now a value of $c=1.373\times 10^{-4}$ mole instead of 1.373×10^{-6} previously) but does not affect the qualitative nature of any of the functions in the previous, or the present model.

The values of the constants used in the simulation are: $c_1=2.24\times 10^4$, $c_2=2.50\times 10^5$, $c_3=8.6\times 10^{10}$, $c_4=1.84\times 10^4$, $c_5=7.36\times 10^6$, $c_6=10.333$, $V_N=0.09$, $V_T=0.05$, $\bar{c}=5$, $c=1.373\times 10^{-4}$, $q_0=0.0122$, $s=1$, $\hat{v}=100$ (max. firing rate), $m=11.25$, $\hat{n}=10$, $k_2=10^{-4}$, $\bar{\delta}=10^{-8}$. The value of ξ was set equal to unity and $\bar{N}$ was changed for different runs.

The equations were coded in ACSL (Advanced Continuous Simulation Language) and integrated on a CDC Cyber 174 digital computer, using a fourth-order Runge-Kutta integration routine.

Figure 1 shows the ε-responses of the exact and the approximating system, for three different values of $\bar{N}$ (5, 10, 20), as well as the functions $\psi(t)$ and $\varphi(t)$, for the control mode described in the legend of Figure 1. Note that the individual motor units of the exact system are recruited sequentially, i. e. for $\bar{N}=20$ the first (smallest) unit comes in at $t=0$, the second at $t=0.005$ s, the third at $t=0.01$ s etc., until the last one is recruited at $t=0.095$ s. Hence at $t=0.1$ (arrow 1) all motor units have been recruited.

It is clearly seen from Figure 1 that the approximation improves rapidly with increasing $\bar{N}$. This is not surprising since the approximating model was derived under the assumption of large values $\bar{N}$. Hence for a muscle having a total of 10 motor units the approximation is good, while for a muscle comprising 20 or more units the approximation is almost perfect. Note the interesting fact that $\varepsilon(t=0.1)$ has a value of only about 0.26 when all the motor units have been recruited (arrow 1 in Fig. 1). This is completely in accordance with the recent experimental findings of Desmedt and Godaux (1977) that in ballistic contractions of the

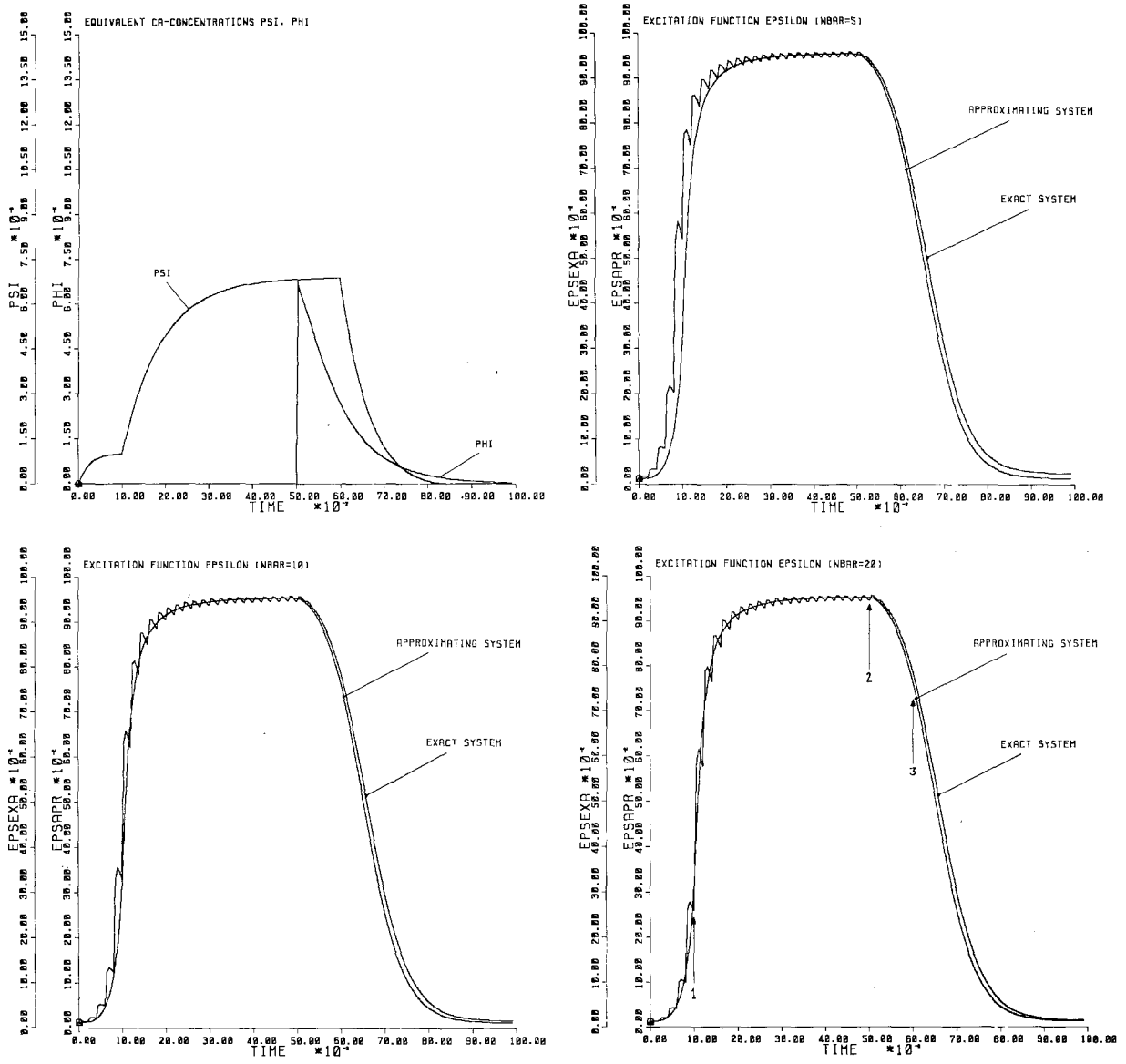

Fig. 1. Equivalent Ca-concentrations $\psi(t)$ and $\varphi(t)$ (in moles), and ε-responses for the exact and approximating system for $\bar{N}=5$ (right upper graph), $\bar{N}=10$ (left lower graph), and $\bar{N}=20$ (right lower graph), for the following control mode: $z=1$ for $0\leqq t\leqq 0.1$, $z=0$ for $0.1<t\leqq 0.5$, $z=-1$ for $0.5<t\leqq 0.6$, $z=0$ for $t>0.6$; $v=0.5$ for all t; time in seconds (note scaling factor of 10^{-2}, i.e. the maximum value is 1 s). The arrows in the lower right-hand graph indicate the switching times of the control z

human tibialis anterior muscle, all the motor units in the muscle have already been recruited at a stage when the force output is still comparatively small.

Figure 2 displays a contractive situation with a completely general control mode described by the control functions $z(t)$ and $v(t)$ shown in the upper part of the figure. In fact, in this simulation the first 14 motor units were controlled by firing rates defined by

$$\begin{aligned} \nu_{1-14}(z,n) &= 83\,\text{Hz} \quad \text{for} \quad z>0 \quad \text{and} \quad n>0.6\,, \\ &= 42\,\text{Hz} \quad \text{for} \quad z\leqq 0 \quad \text{and} \quad n>0.6\,, \\ &= 28\,\text{Hz} \quad \text{for} \quad z\leqq 0 \quad \text{and} \quad n\leqq 0.6\,, \end{aligned}$$

while the last 6 units had rates of

$$\begin{aligned} \nu_{15-20}(z,n) &= 111\,\text{Hz} \quad \text{for} \quad z>0 \quad \text{and} \quad n>0.6\,, \\ &= 56\,\text{Hz} \quad \text{for} \quad z\leqq 0 \quad \text{and} \quad n>0.6\,, \\ &= 37\,\text{Hz} \quad \text{for} \quad z\leqq 0 \quad \text{and} \quad n\leqq 0.6\,. \end{aligned}$$

The normalized average rate $v(t)$ was computed from (32), using these frequencies.

It would appear from the left-hand graph of the lower part of Figure 2 that the approximation for this control mode is not good. However, the picture is misleading for the simple reason that the approximat-

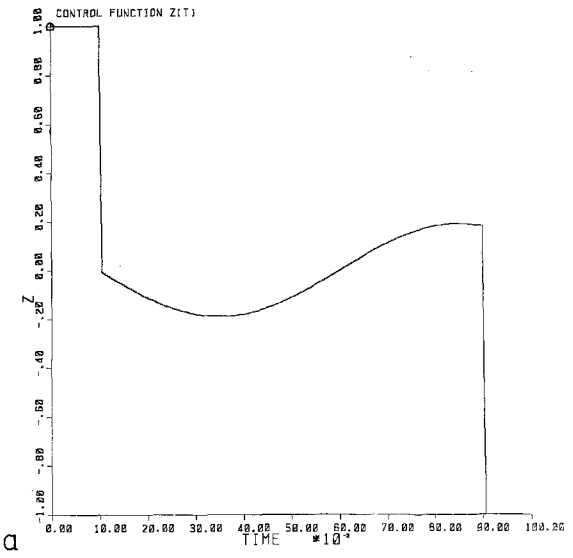

a

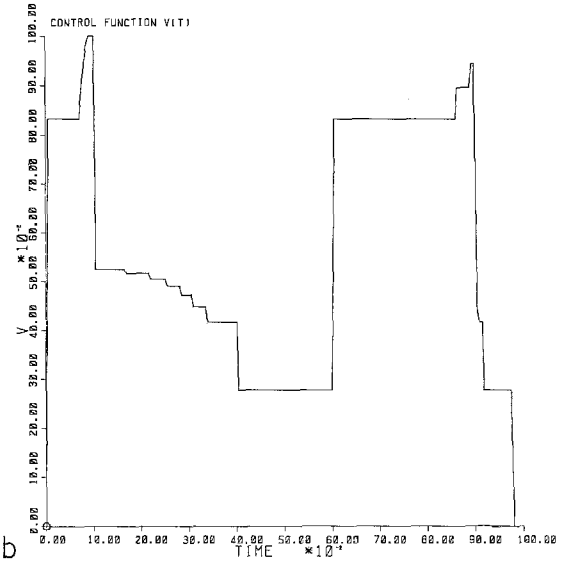

b

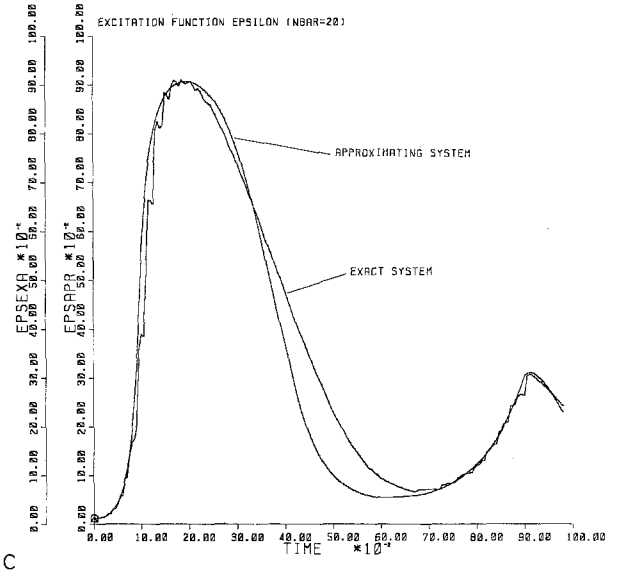

c

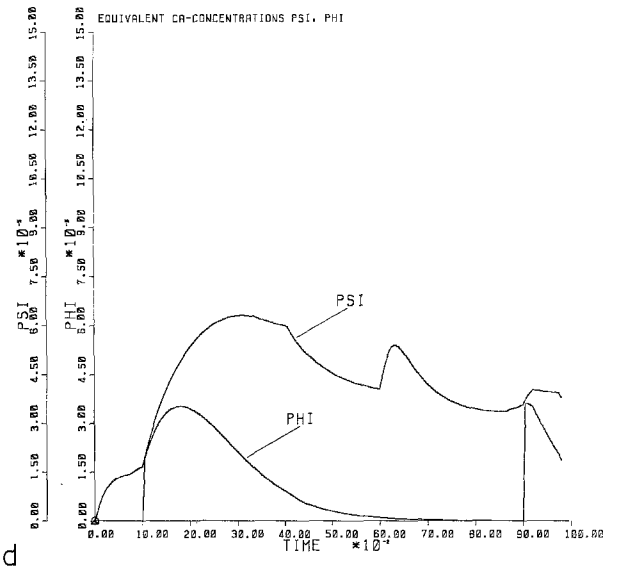

d

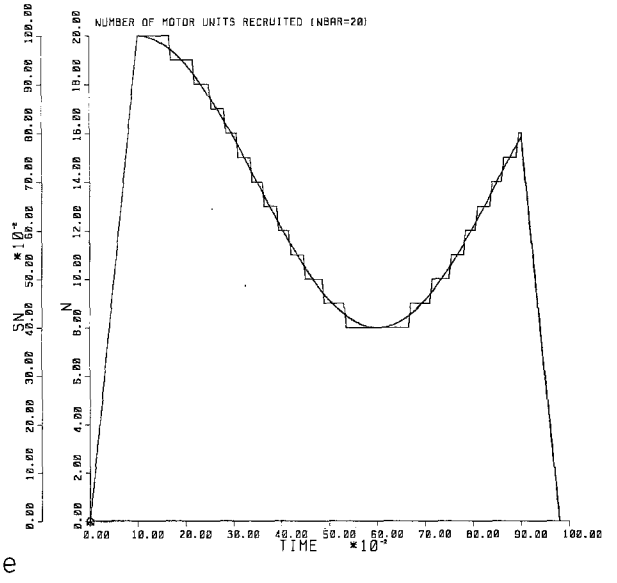

e

Fig. 2a—e. a, b: Control functions $z(t)$ and $v(t)$. **c—e:** ε-responses **c**, equivalent Ca-concentrations **d**, and number of stimulated motor units **e**; $\bar{N}=20$. For detailed explanations see the text

ing system [Eq. (21)] responds immediately to changes in the firing rate, via $v(t)$, while the exact system exhibits a delayed response owing to the fact that a change of the interspike interval [see (31)] manifests itself only at the time of onset of the *next* stimulating pulse. This situation should worsen with increasing interspike interval, i.e. with decreasing firing frequency and should improve with increasing frequency. That this is indeed the case can be seen by comparing the middle parts of the functions $v(t)$ and $\varepsilon(t)$. Thus, accounting for this phenomenon, we are led to conclude that the approximation is reasonable, for this general control mode also.

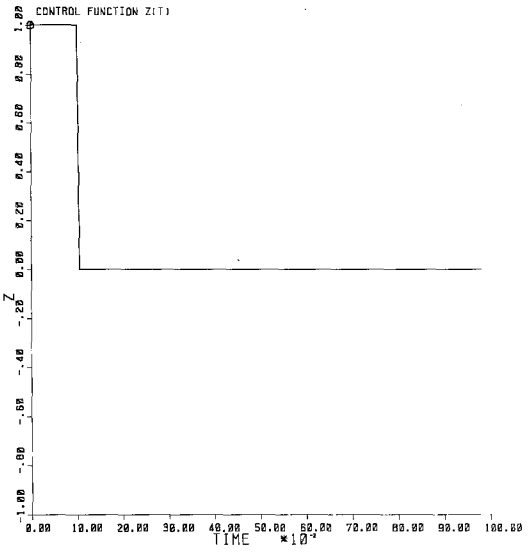

a

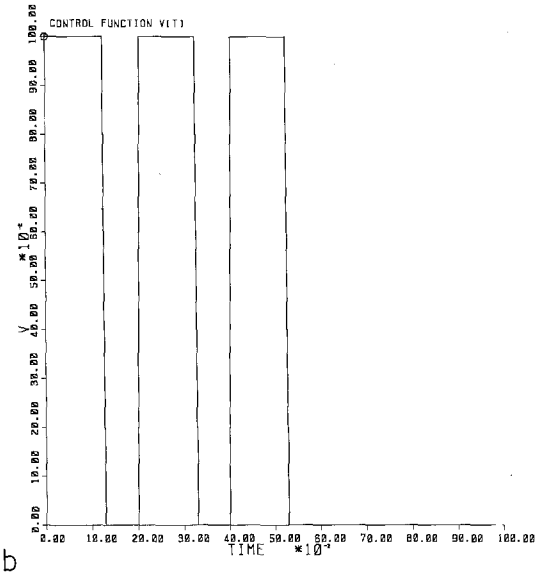

b

Fig. 3a—c. ε-responses **c** to bang-bang type control functions $z(t)$ and $v(t)$ as depicted in **a** and **b** respectively; $\bar{N}=20$

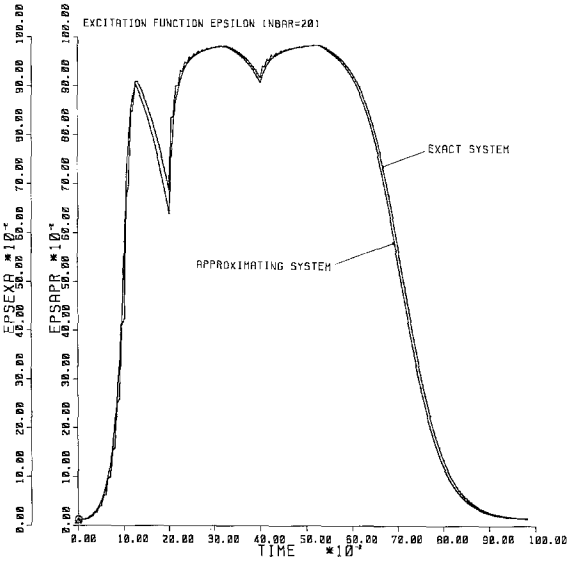

c

Figures 2d and 2e display the corresponding functions $\psi(t)$ and $\varphi(t)$, and the motor unit recruitment patterns of the individual units [step function $N(t)$] and the approximating function [smooth curve $n(t)$], respectively.

Finally, Figure 3c depicts the ε-responses to a typical bang-bang control mode. It is apparent that even under these extreme conditions the approximating model provides a good fit to the exact system.

Although it is obviously impossible to test the model for all conceivable control modes, it is apparent that the model provides good approximations to the responses of the real system under quite general and extreme control conditions. On these grounds, we are justified in having some confidence in the model. However, the final test for a model is always the verification of its predictions. For this reason we shall now use the model for predicting the force output of the human quadriceps muscle group, subject to certain neural control inputs, and compare the predicted force output with the one actually observed on the living system.

Experimental Verification of the Model

An exact description of the experimental methods used will appear elsewhere. Briefly, a male subject (26 years old, 76,4 kg mass, active sprinter and long-jumper) was seated on a special chair with his pelvis belted to the back support. A special force transducer (MFTA-OU-200 load cell), with negligible compliance, was rigidly mounted onto the chair in such a way as to permit the measurement of the isometric force produced by the extensor muscles of the subject's right lower leg. The measurement took place at a distance of 0.36 m below the estimated centre of the knee joint. The knee angle was fixed at $-62°$ with respect to the long axis of the thigh, while the hip was flexed at 61° with respect to the same axis. Surface electromyograms (EMGs) were recorded from m. vastus lateralis, m. rectus femoris, and the hamstring group. The raw EMGs as well as their rectified and smoothed signals (lower cutt-off frequency 6 Hz) were displayed together with the output and the electronically differentiated output of the force transducer on the chart paper of an eight-channel Gould-Brush 481 recorder.

The subject was instructed to produce a certain, near maximal, isometric force in the shortest possible time. It was unimportant whether this target force would be overshot or not, as long as the initial effort was maximal. This mode of contraction was chosen because the neural controls operating under these conditions are fairly well known. In particular, the recent reports of Desmedt and Godaux (1977), and Grimby and Hannerz (1977) have clearly shown that in rapid contractions performed with maximum effort, all stimulated motor units initially fire at their maximum rates (120 Hz and more for fast units) and that these rates quickly decrease to 30–50% of the maximum, presumably when recruitment of all units is

Table 1. Parameter values used in the simulation model (all units in the m-kg-s system, forces in Newtons)

Muscle	$\bar{F}_i$	$\bar{\theta}_i$	$\bar{\zeta}_i$	l_i	$\bar{l}_i$	$\bar{\lambda}_i$	$\bar{l}_{fi}$	a_{1i}	$\bar{\lambda}_{0i}$	q_{0i}	$\hat{v}_i$	$\hat{n}_i$	m_i	$\bar{c}_i$
Slow part of the vasti group ($i=1$)	1376.4	60°	0.085	0.335	0.34	0.034	0.14	3.90	−1.60	0.00082	40	21.10	4.48	3.39
Fast part of the vasti group ($i=2$)	5505.7	60°	0.085	0.335	0.34	0.034	0.14	2.55	−3.40	0.0122	120	44.41	13.44	1.61
M. rectus femoris ($i=3$)	1439.7	70°	0.100	0.536	0.55	0.07	0.07	2.55	−3.84	0.0122	120	14.3	13.44	5

Parameter values which are the same for all three muscles are $\bar{\xi}=0.30$, $\sigma=1.531$, $s=1$, $a_2=0$, $a_6=2.6$, and $c=1.373\times10^{-4}$

complete. In addition, Desmedt and Godaux (1977) have provided evidence (although, in our opinion, not quite conclusive) that the sequential order of recruitment of the motor units, according to their size, is also preserved in these so-called ballistic contractions. Finally, Person and Kudina (1972), and others have shown that motor units are deactivated in reverse order of recruitment.

Hence, accounting for these facts and estimating the firing rates for post-initial contraction phases from the experimental EMG-records, one can hope to obtain a reasonable estimate of the control functions $v_i(t)$, $z_i(t)$, $t\in[0,t_f]$, $i=1,2,3$, which control the force outputs of the slow part of the vasti muscle group ($i=1$), the fast part of this group ($i=2$), and of the rectus femoris muscle (a predominantly fast muscle, $i=3$) respectively. The biomechanical properties of these muscles (ratios of their maximum tetanic forces, length-tension relations, etc.) are also well known from previous exhaustive studies of these muscles by the author (Hatze, 1976). These studies provide estimates for the various parameter values needed in the state and output equations of the model. Table 1 gives a collection of these values as used in the simulation.

Table 1 requires some comments. From the experimental force records and with a moment arm of about 0.04 m for the force of the extensor muscles at the patellar ligament (Smit, 1973; Hatze, 1976) we calculate a maximum tetanic output of 7313 N, 18.5% of which can be attributed to m. rectur femoris and the rest to the vasti group for the particular values of knee and hip angles of the present experiment. The hamstrings were inactive, as is apparent from the EMG records in Figure 4 below. Thorstensson et al. (1976) have taken biopsy specimens from m. vastus lateralis and found that the content of fast fibres in this muscle varies between 39 and 80% of the total fibre content. Considering these proportions to be representative of the whole vasti group, and taking into account that the present subject is a sprinter and long-jumper, we are justified in assuming 20% of the vasti group to consist of slow fibres and 80% of (predominantly) fast fibres. With these data the values of $\bar{F}_i$ in Table 1 can be computed. The values for m_i are found from the relation (Hatze, 1977a)

$$m_i=0.112\hat{v}_i\,, \tag{33}$$

$\hat{v}_i$ being the maximum firing rate of the i-th muscle, while the values for $\bar{c}_i$, $i=1,2,3$ are determined by $\bar{c}_1=\bar{c}+\ln u_1$, $\bar{c}_2=-\ln u_1$, $\bar{c}_3=\bar{c}=5$, where $u_1=0.2$ is the proportion of slow muscle fibres in the vasti group. Finally, the $\hat{n}_i$ are computed from $\hat{n}_1=\hat{n}\bar{c}/\bar{c}_1$, $\hat{n}_1=\hat{n}\bar{c}/\bar{c}_2$, $\hat{n}_3=\hat{n}=14.3$. Note that $\bar{c}_1+\bar{c}_2=\bar{c}_3$ and $1/\hat{n}_1+1/\hat{n}_2=1/\hat{n}_3$, i.e. the slow and fast parts of the vasti group are taken together as one muscle which obeys the same recruitment dynamics as m. rectus femoris.

The constants b_{1i} and b_{2i}, $i=1,2,3$ can be computed from a_{1i} and a_{2i} (Hatze, 1977a) while the initial conditions ξ_{0i} are determined by $\dot{\xi}(0)=0$ in the last of (21). The length-tension relations $k_i(\xi_i)$, $i=1,2,3$, for the three muscles are as given in Hatze (1976).

The total force output of m. quadriceps femoris is obviously given by the sum of the forces contributed by the individual muscles, i.e.

$$F(t)=F_1^{SE}(t)+F_2^{SE}(t)+F_3^{SE}(t)\,,\quad t\in[0,t_f]\,, \tag{34}$$

where $F_i^{SE}(t)$, $i=1,2,3$, is given by (4) with the expressions for penniform muscles substituted into it. Forces due to passive structures spanning the hip and knee joint are negligible for the specific hip and knee angles chosen (Hatze, 1976). The functions $\xi_i(t)$, $i=1,2,3$, which appear in (4) are determined by the contraction and excitation dynamics of system (21). The simulation was performed on a CDC Cyber 174 digital computer using the simulation language ACSL.

A typical contraction record and its simulation are shown in the left and right-hand graphs of Figure 4 respectively.

For an explanation of the various displays see the legend of Figure 4. The control inputs $v_i(t)$ and $z_i(t)$, $i=1,2,3$, to the simulation model were estimated from the respective raw-EMG records, as outlined above. The functions $v_i(t)$ are as illustrated in Figure 4 [note that the EMG record for the vasti group corresponds approximately to the composite of $v_1(t)$ and $v_2(t)$] while the controls $z_i(t)$ are given by

$$\begin{aligned}
z_1(t) &= 1 \quad \text{for} \quad 0\leqq t<0.0474\\
&= 0 \quad \text{for} \quad 0.0474\leqq t<0.5525\\
&= -1 \quad \text{for} \quad 0.5525\leqq t<0.6000\\
&= 0 \quad \text{for} \quad t>0.6000\,,\\
z_2(t) &= 0 \quad \text{for} \quad 0\leqq t<0.0474\\
&= 1 \quad \text{for} \quad 0.0474\leqq t<0.070\\
&= 0 \quad \text{for} \quad 0.070\leqq t<0.530\\
&= -1 \quad \text{for} \quad 0.530\leqq t<0.5525\\
&= 0 \quad \text{for} \quad 0.5525\leqq t\,,
\end{aligned}$$

and

$$\begin{aligned}
z_3(t) &= 1 \quad \text{for} \quad 0\leqq t<0.070\\
&= 0 \quad \text{for} \quad 0.070\leqq t<0.530\\
&= -1 \quad \text{for} \quad 0.530\leqq t<0.6000\\
&= 0 \quad \text{for} \quad 0.6000\leqq t\,.
\end{aligned}$$

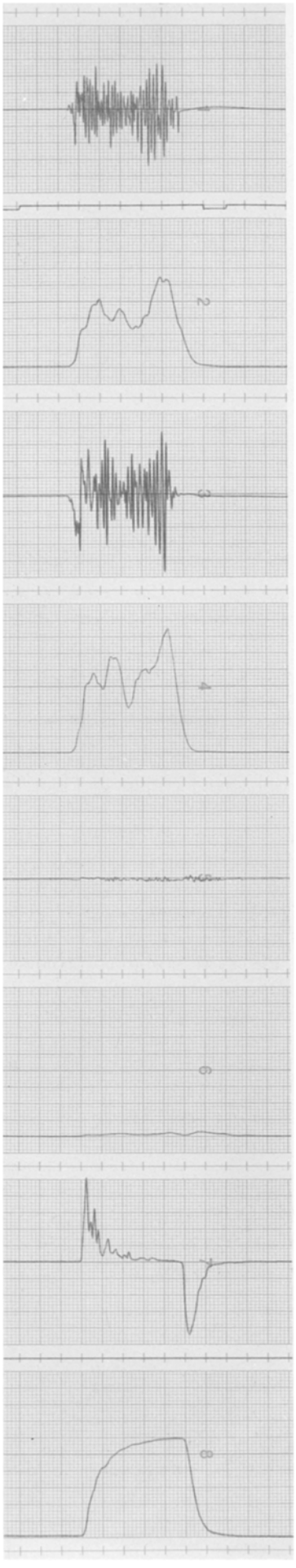

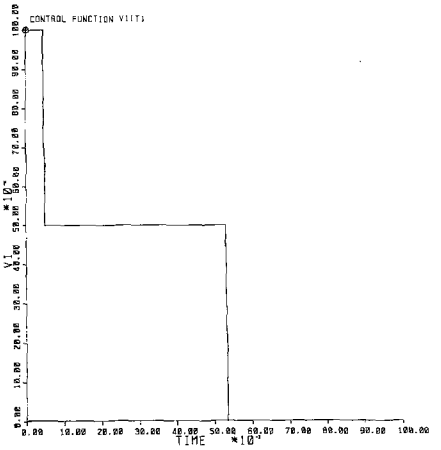

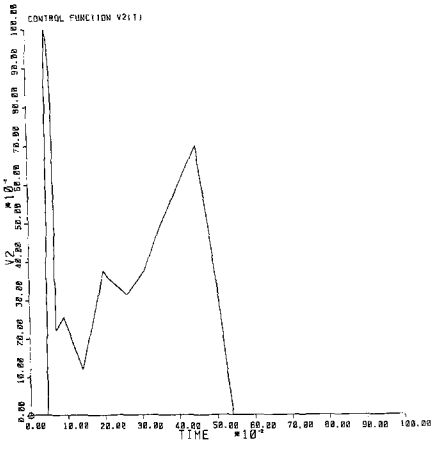

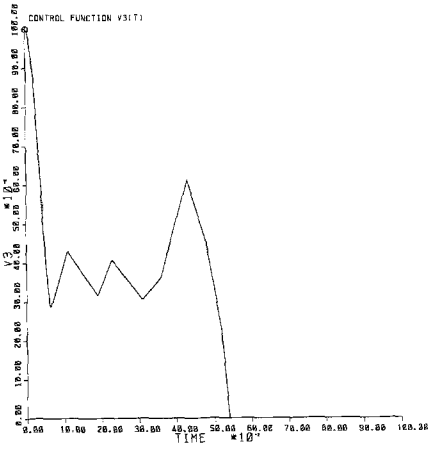

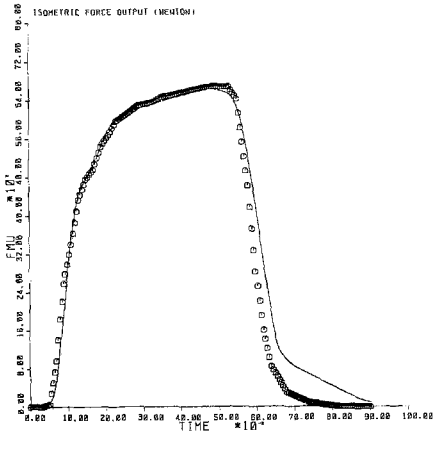

Fig. 4. *Left-hand part.* From top: raw EMG and rectified and smoothed EMG from m. rectus femoris respectively, same two signals from m. vastus lateralis (below rectus femoris), and hamstring group (below vastus lateralis). The last two records display the differentiated force output and the isometric force output (lowest record) respectively. Force scale: 1125 *N*/large division. *Right-hand part.* From top: control functions $v_i(t)$, $i=1,2,3$, and model force output $F(t)$ (continuous line) respectively. For comparison, the experimental results (FMU) of the muscle's force output, as shown in the lowest record on the left-hand side of the figure, are depicted as the symbols. Note that the control functions $v_i(t)$ are not directly related to the EMG records opposite them on the left (for details see the text)

Note that recruitment in this maximum-effort contraction is complete in 70 ms in both muscles and that deactivation of motor units, in reverse order of recruitment, begins at $t=0.53$ s.

The lower right-hand part of Figure 4 depicts the predicted force output $F(t)$ of the model (continuous line) and is compared with the actual force output FMU (symbols) of the m. quadriceps femoris of the subject as given by the force record in the lower left-hand part of the figure. On the whole, the agreement between model prediction and experimental result is quite good except for discrepancies in the early part of the force rise and the declining phase of the force record. The nature of these discrepancies suggests that the estimated value $u_1=0.2$ for the proportion of slow motor units in the m. vastus of this specific subject is too high. Simulation runs with smaller values of u_1 were then performed which confirmed this conjecture. Indeed, with a value of $u_1=0.07$ or less the model response coincides almost perfectly with the experimental record. However, since no muscle biopsies were taken from the subject, the exact value of u_1 remains uncertain and it was, therefore, decided not to depart from the original estimate of $u=0.2$. After all, it is not the purpose of this investigation to produce "nice-looking" curves but to critically scrutinize the properties of the model.

Some of the model predictions are indeed remarkable. The well-known delay of about 50 ms which exists between the onset of the excitation and that of contraction is correctly predicted by the model (Fig. 4). The significance of this feature is that by analyzing the model structure we are able to give an explanation of this phenomenon. However, such an analysis is beyond the scope of this paper and will, therefore, appear elsewhere. Another interesting feature of the model is the prediction of the "dips" occurring in the force records. These dips are due to the firing in "bursts" and the synchronization of motor units. Note that the synchronization frequency is about 8 Hz for the fast units of m. vastus lateralis, and about 10 Hz for m. rectus femoris. Again, a detailed account of these phenomena will be given elsewhere.

The predictions of the present model as well as our experimental results and those of many other investigators in this field are contradicted by the predictions of a muscle model recently proposed by FitzHugh (1977). We shall comment on this discrepancy in the next section.

The main purpose of this section was to verify the present model by demonstrating that it is indeed capable of correctly predicting the various experimentally observed phenomena of muscular contraction mentioned above.

A discussion of the special features of this general model follows in the next section.

Discussion of the Model

The general myocybernetic model as developed and tested in this report is distinctly superior to the previous model in a number of respects.

First and most important, the restriction to constant values of the number of stimulated motor units has been removed and the new model permits the full range of possible control modes. Indeed (as was to be expected) the previous model emerges as a special case of the present general model. To show this, assume that the muscle was in its resting state when it had been excited by some controls $z(t)>0$, $v(t)>0$, $t\geqq 0$. At some time $t_1>0$ we put $z(t)\equiv 0$ for all $t\geqq t_1$, i.e. we terminate recruitment and hence keep $n=n_1$ constant. By (22) and (10) this implies a constant value of $u=u_1$. Consider the state of the system (21) at a time $t'\gg t_1$, i.e. the steady state with respect to the dynamics induced by the control z alone. Then it follows from (21) that $n(t')=n_1$, $r(t')\approx 0$, $\dot{\psi}=m(cv-\psi)$, $\varphi(t')\approx 0$; the last of (21) remains unchanged. By substituting γ for ψ it is seen that (21) reduces to the excitation and contraction dynamics of the previous model (1) with ε eliminated as a state.

We still have to show that for the above steady-state condition the excitation function ε, as given by (28), degenerates to the function ε, expressed by (6), of the previous steady-state model. Now, since $r=0$, $n=n_1$, $\psi=\gamma$, and $\varphi=0$ in (28), and by virtue of (10) and the relation $\bar{c}=-\ln u_0$, it is readily shown that (28) becomes

$$\varepsilon=\{u_1[q(\xi,\gamma(v,t))-q_0] + q_0-u_0 q(\xi,\gamma(v,t))\}/[1-u_0]\,, \tag{35}$$

which is seen to be identical with (6) if we put $u_0=0$. While in the previous model a value of $u_0=0$ was permissible, this is no longer the case for the general model, as is obvious from (10). The reason is that u_0 represents the relative size of the smallest motor unit in the general model, which clearly implies $u_0>0$. However, the value of u_0 is about 0.007 so that (35) is in any case approximately equal to (6). This proves that the previous model emerges as a special case of the new general model.

A second characteristic in favour of the new model is that no more stiffness problems are experienced, a fact which greatly facilitates the numerical integration of the state equations. The same remark applies to the previous model (1) when ε is eliminated as a state [see (7)–(9)].

There is, however, one restriction on the way in which the control z in the general model may vary. For reasons given in the Appendix, the control $z(t)$ may not alternate in sign too rapidly. For some control modes this restriction may become important.

One point regarding the active state function $q(\xi,\gamma)$, as given by (9), must be strongly emphasized since it has

given rise to unfortunate misunderstandings. Calvert and Chapman (1977) have commented on the model of Hatze (1977a) stating that we have "chosen to identify active state with intracellular calcium concentration". This unfortunate misinterpretation entirely misses the point, since we have quite clearly postulated that "we define the active state q to be the *relative amount of* Ca *bound to troponin*" (Hatze, 1977a, p. 106). Now, the intracellular calcium concentration to which Calvert and Chapman refer is given by the function $\gamma(t)$, as defined by (1). The important point to realize is that $\gamma(t)$ is, in fact, an *input* to the active state function $q(\xi, \gamma)$ and by no means the active state itself. Indeed, the highly nonlinear relationship existing between the Ca concentration γ and the active state q constitutes one of the most remarkable biochemical properties of the myostructures. As clearly demonstrated in Figure 4 of Hatze (1977a), the active state function $q(\xi, \gamma)$ exhibits a saturating behaviour for large values of γ. This property enables the active state to rise much faster upon stimulation than would be possible if q were a linear function of $\gamma(t)$. Expressed differently: even a comparatively low Ca concentration γ is sufficient to expose a large number of potential interactive sites on the troponin-tropomyosin complexes attached to the actin filaments. The actomyosin cross-links, which then form at these desinhibited locations, are responsible for the production of contractive force [for a detailed discussion and references see Hatze (1977a)].

As is apparent from the first of Equations (1) the rate of rise of the Ca concentration $\gamma(t)$ itself is controlled by the relative stimulation rate v and by the value of the constant m. Hence large values of m (fast muscles) and v imply fast rises of $\gamma(t)$. It has been suggested (Kernell, 1965) that the initial steep portion of the active state curve corresponds to the primary range of firing frequencies of the motorneurons innervating the muscle, while the portion of saturation corresponds to the secondary firing range. This would explain the sudden change in the slope of the "frequency-current" curves of the motorneurons (Kernell, 1965).

These remarks should clarify the connection between the Ca concentration γ and the active state $q(\xi, \gamma)$.

Finally, we must explain the serious discrepancies between the predictions of the present control model and that of FitzHugh (1977). Since our excitation function $\varepsilon(t)$ [see (28)] has its exact counterpart in the control function $U(t)$ of FitzHugh's model (both functions multiply the output of the contractile element) the patterns of the two functions for various control modes can be compared. For a bang-bang control input, $v(t)$, our excitation function $\varepsilon(t)$ exhibits the behaviour shown in Figure 3 while for this case FitzHugh's control $U(t)$ (which is some undefined function of the stimulation rates) is identical with our bang-bang control $v(t)$. As can be seen, the patterns of these two functions are fundamentally different. In fact, since our excitation function ε and FitzHugh's control U are equivalent to the active state (in A.V. Hill's sense) of the contractile element, FitzHugh's model implies that the active state can change in a bang-bang form. This is clearly demonstrated by his predictions of "optimal" active state functions which exhibit discontinuous switchings for various nonisometric contractions [lowest curves in Figure 2 of FitzHugh (1977)]. It is obvious that such a model contradicts the well-known phenomena of the excitation dynamics of skeletal muscle. In particular, the model violates all experimentally established facts about the time course of the active state (Bahler et al., 1967; Ebashi and Endo, 1968; Jewell and Wilkie, 1960; etc.), the dynamics of the sarcoplasmic calcium release upon stimulation (Jöbsis and O'Connor, 1966), the highly nonlinear dependence of the active state on the intracellular Ca concentration (Ebashi and Endo, 1968; Julian, 1971), etc. Indeed, a scrutiny of FitzHugh's model reveals that as far as the inclusion of the control parameter U is concerned, the model is an exact copy of Stark's (1968) muscle model, with U replacing Stark's control α, while FitzHugh's optimal control treatment of his muscle model is in most respects a mere restatement of the methods suggested by Chow and Jacobson (1971), and Hatze (1976). Also, FitzHugh's assumptions regarding the linear dependence of the heat rates on the control U directly contradict the experimental findings of Gibbs and Gibson (1972), Julian (1971), Wendt and Gibbs (1973), and others.

These deficiencies in the structure of FitzHugh's model explain the discrepancies existing between the predictions of the model and the experimentally established facts of muscular contraction.

Although attempts to develop adequate control models of skeletal muscle can only be commended, it is nevertheless also true that oversimplified models can do more harm than good. There are indications that physiologists and experimental biologists are also beginning to recognize myocybernetics, the discipline concerned with the discovery and cybernetical description of optimality principles operating in the neuromuscular control system; however, predictions of optimal neuromuscular behaviour, based on models which grossly contradict physiological reality, can only serve to undermine the credibility of this youthful discipline.

Appendix

Derivation of the State Equations for the General Model

Let the time interval between the recruitment, at times t_N and t_{N+1}, say, of the N-th and the $(N+1)$-st motor units respectively, be

$\Delta t(t) \triangleq t_{N+1} - t_N$. Since the total number $\bar{N}$ of motor units present in a muscle is usually large (hundreds to thousands) we are justified in approximating the step function $N(t)/\bar{N}$, $0 \leqq t \leqq T$, by the *absolutely continuous* and *piecewise differentiable* function $n(t)$, defined by

$$\dot{n}(t) \triangleq \hat{n}z(t) \triangleq [N(t+\Delta t(t)) - N(t)]/\bar{N}\Delta t(t) = 1/\bar{N}\Delta t(t) , \quad n(0) = 0 , \quad 0 \leqq n \leqq 1 , \tag{A1}$$

where $z(t)$, $-\check{z} \leqq z(t) \leqq 1$, and hence $\dot{n}(t)$, $t \in [0, T]$, are *piecewise constant* functions of t. For the definition of all the symbols see the main text.

From (A1) it follows that

$$\Delta t(t) = 1/[\bar{N}\hat{n}z(t)] , \tag{A2}$$

where $z(t) \neq 0$ is constant for $t_N \leqq t \leqq t_N + \Delta t(t)$, $N = 1, 2, \ldots$, and $\hat{n}$ denotes a constant.

Assume that at the time t_i of stimulation there is a rest Ca-concentration $\varphi(t)$ in the i-th motor unit and that the control $v_i(t)$ of this unit is constant for $t \in [t_i, t_i + \Delta_i t)$. Then $\gamma_i^+(v_i(t-t_i))$ appearing in (15) can be found by integrating the first of Equations (1):

$$\gamma_i^+(v_i(t-t_i)) = cv_i[1 - \exp\{-m_i(t-(i-1)\Delta t(t))\}] + \varphi(t) , \tag{A3}$$

with $\Delta t(t)$ given by (A2), and m_i indicating that m may be different for each unit.

Dealing with $\varepsilon^+(t)$ first, our objective is to find a function $\psi(\cdot)$ such that (19) is a sufficiently accurate approximation to (15). Since $\bar{N}$ is large, we may use an integral approximation to the sums, so that we require

$$q(\xi, \psi(v,t)) \int_1^{N(t)} \exp(\bar{c}x/\bar{N})dx = \int_1^{N(t)} \exp(\bar{c}x/\bar{N}) q(\xi, \gamma^+(t,x))dx ,$$

or, by putting $\bar{c}x/\bar{N} = \tau$ [so that, by (A2), $x\Delta t(t) = \tau/\bar{c}\bar{N}z(t)$], and integrating the left-hand side,

$$[\exp(\bar{c}n(t)) - \exp(\bar{c}/\bar{N})] q(\xi, \psi(v,t)) = \int_{\bar{c}/\bar{N}}^{\bar{c}n(t)} \exp(\tau) q(\xi, \gamma^+(t,\tau))d\tau . \tag{A4}$$

It can be shown that the function $q(\xi, \gamma)$ given by (9) can be approximated reasonably accurately by the function

$$\tilde{q}(\xi, \gamma) = 1 - (1 - q_0)\exp(-\varrho_0(\xi)\gamma) , \tag{A5}$$

where $\varrho_0(\xi)$ is given by (24). This approximation will enable us to derive a differential equation for ψ. By using this approximation in (A4), assuming $\bar{N}$ sufficiently large for the terms containing the factor $1/\bar{N}$ to be negligible, and comparing left and right-hand sides of the resulting equation, we find that $\psi(v,t)$ must satisfy

$$[\exp(\bar{c}n(t)) - 1]\exp\{-\varrho_0(\xi)(\psi(v,t) - \varphi(t))\} = \int_0^{\bar{c}n(t)} \exp\{\tau - \varrho_0(\xi)cv(t) \cdot (1 - \exp[-m(\tau)(t - \tau/\bar{c}\hat{n}z(t))])\}d\tau , \tag{A6}$$

where (A3) has been substituted into (A4), and use has been made of (A2) and the transformation $\bar{c}x/\bar{N} = \tau$. The quantity ξ (here a parameter) is also assumed to be piecewise constant on the same interval as z, and $v(t)$ constitutes an "average" stimulation rate (averaged over N) as defined in model (1).

Generally, there is no hope of obtaining a non-differential analytical expression for $\psi(\cdot)$ from (A6) which does not contain the integral, not even for constant v and z. However, it is possible to derive a differential equation for ψ which no longer contains the integral.

To this end, let it be assumed that $v(t)$ is piecewise constant on the same interval as $z(t)$ (it will be seen below that this assumption is not as restrictive as might appear). Let, therefore, v and z have the constant values v_1 and z_1 on the interval $[0, t_1)$. Owing to the stipulation of piecewise constancy for ξ we can write ϱ_0 for $\varrho_0(\xi)$ on $[0, t_1)$. From the structure of (A6) we can infer that $\psi(v_1, t)$ will be of the form

$$\psi(v_1, t) = cv_1(1 - g(t)) , \tag{A7}$$

which, when substituted into (A6), yields

$$[\exp(\bar{c}n(t)) - 1]\exp\{\varrho_0(cv_1 g(t) + \varphi(t))\} = \int_0^{\bar{c}n(t)} \exp\{\tau + \varrho_0 cv_1 \exp[-m(\tau)(t - \tau/\bar{c}\hat{n}z_1)]\}d\tau , \tag{A8}$$

after cancellation of the term $\exp(-\varrho_0 cv_1)$.

Differentiating (A8) with respect to t, and noting that $dn/dt = \hat{n}z_1$, we have

$$\begin{aligned} &\bar{c}\hat{n}z_1 \exp\{\bar{c}n + \varrho_0(cv_1 g + \varphi)\} + \varrho_0(cv_1\dot{g} + \dot{\varphi})I \\ &= \bar{c}\hat{n}z_1 \exp(\bar{c}n + \varrho_0 cv_1) \\ &\quad - \varrho_0 cv_1 \int_0^{\bar{c}n} m(\tau)\exp\{-m(\tau)(t - \tau/\bar{c}\hat{n}z_1) \\ &\quad + \tau + \varrho_0 cv_1 \exp[-m(\tau)(t - \tau/\bar{c}\hat{n}z_1)]\}d\tau , \end{aligned} \tag{A9}$$

where I is the integral (A8). A second differentiation of (A8) with respect to v_1 yields

$$Ig = \int_0^{\bar{c}n} \exp\{-m(\tau)(t - \tau/\bar{c}\hat{n}z_1) + \tau + \varrho_0 cv_1 \exp[-m(\tau)(t - \tau/\bar{c}\hat{n}z_1)]\}d\tau .$$

By putting $\bar{c}n = \tau$ on the left (in the expression for I) and right-hand sides of this relation, and changing the dummy variable to y, the above expression can be written as

$$I(\tau)g = J(\tau) , \tag{A10}$$

where $J(\tau)$ represents the integral on the right-hand side.

An integration by parts of the integral K appearing on the right-hand side of (A9) yields

$$K = [m(\tau)J(\tau)]_0^{\bar{c}n} - \int_0^{\bar{c}n} J(\tau)dm(\tau) = g\left[m(\bar{c}n)\exp(\bar{c}n) - m(0) - \int_0^{\bar{c}n} \exp(\tau)dm(\tau)\right] \cdot \exp[\varrho_0(cv_1 g + \varphi)] ,$$

where (A10) and (A8) have been used. This expression for the integral K may now be substituted into (A9); and by virtue of the relations $cv_1\dot{g} = -\dot{\psi}$, and $cv_1 g = cv_1 - \psi$ [see (A7)], we find, by putting

$$m(n) \triangleq \left[m(\bar{c}n)\exp(\bar{c}n) - m(0) - \int_0^{\bar{c}n} \exp(\tau)dm(\tau)\right] \Big/ [\exp(\bar{c}n) - 1] , \tag{A11}$$

that

$$\dot{\psi} = m(n)(cv_1 - \psi) + \bar{c}\hat{n}z_1[1 - \exp\{\varrho_0(\psi - \varphi)\}]/\varrho_0[1 - \exp(-\bar{c}n)] + \dot{\varphi} , \tag{A12}$$

where $\varphi(t)$ is an, as yet unspecified, absolutely continuous and piecewise differentiable function. If $m(n) = m$ is a constant, then $dm(\tau) \equiv 0$ and (A11) reduces to m. Although we have succeeded in finding an equation for $\dot{\psi}$ which includes the effect of a varying motor unit parameter m this is, unfortunately, not of much use since (13) was derived under the assumption of constant motor unit parameters which relate to the contraction dynamics. Without this assumption,

the treatment becomes too complicated and no useful results can be derived. Thus we shall, from now on, restrict ourselves to the case where m is a constant.

Equation (A12) is the required differential equation for ψ, subject to constant controls v_1, z_1, and with a constant value ϱ_0 on the interval $[0, t_1)$. It can easily be shown that the solutions $\psi(t)$ and $\varphi(t)$, $t\in[0,\infty)$, of (A12) and (A16) below are bounded such that

$$0\leqq\psi(t),\varphi(t)\leqq c\,,\quad t\in[0,\infty)\,. \tag{A13}$$

This implies that no finite escape times exist for these solutions, which permits us to *define* the values of $\psi(t)$ and $\varphi(t)$, at the switching time t_1, as the continuation of the solutions for $t<t_1$ (Coddington and Levinson, 1955). Thus if at time t_1 the controls v and (or) z switch discontinuously to new constant values v_2 and z_2, Equations (A12) and (A16) below can be integrated over $[t_1, t_2)$ using the new initial conditions $\psi(t_1)$, $\varphi(t_1)$, even though the right-hand sides of the respective differential equations do not exist at $t=t_1$. By continuing in this fashion the global solutions $\psi(t)$ and $\varphi(t)$ are obtained. For obvious reasons the index 1 on z_1 and v_1 may now be dropped and Equation (A12) will be stated in its final form once an expression for $\dot\varphi(t)$ has been derived.

Equation (A12) holds true strictly only for $z\geqq 0$ because it contains the specific recruitment history as specified by (A3). It can, however, be shown that this influence of control history on present values of the state variables quickly fades out so that the model (A12) remains valid also for $z<0$, with z equated to zero in (A12), *provided $z(t)$ does not alternate in sign too rapidly*. This theoretical result is also borne out by the simulation responses (Figs. 1–3). It should, however, be kept in mind that the system is, basically, a *hereditary* one but that a proper consideration of this fact would lead to almost unmanageable complexity.

We turn now to $\varepsilon^-(t)$, i.e. to the derivation of the equation for $\varphi(t)$. We seek a function $\varphi(\cdot)$ such that (20) is a sufficiently accurate approximation to (16). In analogy to (A3) we have

$$\gamma_j^-(t)=\psi(t)\exp[-m(t-(j-1)\Delta t(t))]$$

and by following the same procedure which led to (A6) we obtain

$$\begin{aligned}&[1-\exp(-\bar c r(t))]\exp\{-\varrho_0(\xi)\varphi(t)\}\\&\quad=\int_0^{\bar c r(t)}\exp\{-\tau-\varrho_0(\xi)\psi(t)\exp[-m(t-\tau/\bar c\,\hat n(-z))]\}d\tau\,,\end{aligned} \tag{A14}$$

where t is counted from the time when z became negative (switching off of motor units), and $r(t)$ is obviously given by

$$\dot r=-\dot n=-\hat n z(t)\,,\quad r(0)=0\,,\quad 0\leqq r\leqq 1\,. \tag{A15}$$

Equation (A14) arises from the fact when a motor unit is switched off it is transferred from the N-population of stimulated units to the R-population of semi-active units and its initial concentration $\psi(t)$ begins to decline exponentially according to $\psi\exp(-mt)$. The same process applies to the next unit but with a time delay of Δt. Carrying on in this way and summing the corresponding active states, we obtain the integral expression (A14).

Equation (A14) is first differentiated with respect to t (again holding ξ constant) and then with respect to $\varrho_0(\xi)$. Proceeding in the same way as with (A9) we find

$$\begin{aligned}\dot\varphi&=-\varphi m+\dot\psi\varphi/\psi\\&\quad-\bar c\hat n z[1-\exp\{\varrho_0(\xi)(\varphi-\psi)\}]/\varrho_0(\xi)[\exp(\bar c r)-1]\,,\end{aligned} \tag{A16}$$

where $\dot\psi=m(cv-\psi)$ [from (A12)] for $z<0$.

When $z\geqq 0$, no units are transferred from the N-population to the R-population and hence $\dot\varphi=-\varphi m$, i.e. φ declines exponentially.

From the preceding discussion on the domains of validity of the Equations (A12) and (A16) it is clear that we need a *switching function* $w(z)$ which switches parts of the equations on or off, depending on the value and sign of the control z. Let $w(z)$ be defined by (26), and w^+ and w^- by (25). Then it follows that (A12) can [by virtue of (A13) and its implications] be written as

$$\begin{aligned}\dot\psi&=m(cv-\psi)+w^+z\bar c\hat n[1-\exp\{\varrho_0(\xi)(\psi-\varphi)\}]/\varrho_0(\xi)\\&\quad\cdot(1-\exp(-\bar c n-\bar\delta))-(1+w^-)\varphi m\,,\quad\psi(0)=0\,,\end{aligned} \tag{A17}$$

and (A16) as

$$\begin{aligned}\dot\varphi&=-\varphi m-w^-\{m(cv/(\psi+\bar\delta)-1)\varphi\\&\quad-z\bar c\hat n[1-\exp\{\varrho_0(\xi)(\varphi-\psi)\}]/\varrho_0(\xi)(\exp(\bar c r+\bar\delta)-1)\}\,,\\&\quad\varphi(0)=0\,,\end{aligned} \tag{A18}$$

since $\dot\psi\varphi/\psi=m(cv-\psi)\varphi/\psi$ for $z<0$. It is seen that (A17) and (A18) are identical with the third and fourth of (21). Note that the small constant $\bar\delta$ (value about 10^{-8}) has been added to the respective variables in order to obviate division by zero when $n=0, r=0, \psi=0$. It can be shown that this procedure does not significantly influence the accuracy of the solution, provided $\bar\delta$ is chosen sufficiently small. Computational difficulties, which are due to the fact that $\psi>0$ but $\varphi=0$ in the last term of (A18) when w^- becomes -1 for the first time, can be obviated by simply setting $\varphi(t_s)=\psi(t_s)$ at the switching time t_s and then integrating in the normal way. After all, the difficulties arise only because $\varphi(t_s)$ should attain the value $\psi(t_s)$ in an infinitely short period of time.

Finally, we have to derive the differential equation defining $r(t)$. Basically, this differential equation is given by (A15), but contradictions arise when during a contractive situation $\varphi>0, r>0$, but z becomes zero and remains zero for a longer period of time. Then $\varphi(t)$ declines exponentially [by (A18)] but $r(t)$ remains constant [by (A15)] although, after some time, φ will be practically zero and hence r (the normalized population of semi-active motor units) should also be zero. This problem can be overcome by *defining* a unit to be *inactive* if φ becomes smaller than a certain threshold value k_2c, i.e. we require that

$$k_2c=\varphi\exp(-m\hat t)\,, \tag{A19}$$

where $\hat t$ is related to the "cut-off value" $\hat r$ by

$$\hat t\triangleq\hat R\Delta t=\hat r/\hat n(-z)\,. \tag{A20}$$

For $z\geqq 0$ we want $r(t)$ to decline exponentially, just as $\varphi(t)$ does. Hence we augment (A15) by the term $(1+w^-)m'r$, i.e. (A15) becomes

$$\dot r=-\hat n z-(1+w^-)m'r\,, \tag{A21}$$

where the last term is nonzero only for $z\geqq 0$, and m' is to be determined. Now, if $r=\hat r$ then we must have $\dot r=0$, i.e.

$$m'=-\hat n z/\hat r=1/\hat t=m/\ln(\Delta+\varphi/k_2c)\,, \tag{A22}$$

where (A19)–(A21) have been used and a suitably small constant Δ has been added to provide for the case when $\varphi=0$. It is not difficult to show that $\Delta=1+10^{-3}$ m, and $k_2=10^{-4}$ constitute appropriate choices for the respective constants. In fact, with the above value for k_2, we have $k_2c=1.373\times10^{-8}$ mole which is just the resting Ca-concentration in the muscle (Ebashi and Endo, 1968), i.e. a motor unit is declared inactive when its Ca-concentration has reached the actual physiological resting value.

A final point must be clarified. It is seen that upon integrating (A15) from $t=0$ (where $z>0$) to some t, the constraint on r is violated, since r will become negative. This can be prevented, without significantly affecting the accuracy of the solution, by simply multiplying $z(t)$ by $(r-w^-\bar\delta)/(r+\bar\delta)$, $\bar\delta=10^{-8}$ (say). This procedure also removes the constraints on r.

With (A22) substituted into (A21) the final differential equation for r thus becomes

$$\begin{aligned}\dot r&=-\hat n z(r-w^-\bar\delta)/(r+\bar\delta)-(1+w^-)mr/\ln(1+10^{-3}m+\varphi/k_2c)\,,\\&\quad r(0)=0\,,\end{aligned} \tag{A23}$$

which, together with (A1), constitutes the recruitment dynamics [the first two of Equations (21)]. Note also that the augmented Equation (A23) does not contradict (A15), which was used in the derivation of (A16) for $z<0$, since for this case (A23) reduces to (A15).

This completes the derivation of the model equations.

Acknowledgement. Thanks are due to Prof. K.C. Hayes and Miss Karen Robinson of the Department of Kinesiology of the University of Waterloo, Canada, for valuable assistance in carrying out the experiments.

References

Bahler, A.S., Fales, J.T., Zierler, K.L.: The active state of mammalian skeletal muscle. J. gen. Physiol. **50**, 2239—2253 (1967)

Briggs, F.N., Poland, J.L., Solaro, R.J.: Relative capabilities of sarcoplasmic reticulum in fast and slow mammalian skeletal muscles. J. Physiol. **266**, 587—594 (1977)

Calvert, T.W., Chapman, A.E.: The relationship between the surface EMG and force transients in muscle: simulation and experimental studies. Proc. IEEE **65**, 682—689 (1977)

Chow, C.K., Jacobson, D.H.: Studies of human locomotion via optimal programming. Math. Biosci. **10**, 239—306 (1971)

Coddington, E.A., Levinson, N.: Theory of ordinary differential equations (pp. 13—61). New York: McGraw-Hill 1955

Desmedt, J.E., Godaux, E.: Ballistic contractions in man: characteristic recruitment pattern of single motor units of the tibialis anterior muscle. J. Physiol. **264**, 673—693 (1977)

Ebashi, S., Endo, M.: Calcium and muscle contraction. Progr. Biophys. **18**, 123—183 (1968)

Edman, K.A.P., Mulieri, L.A., Scubon-Mulieri, B.: Non-hyperbolic force-velocity relationship in single muscle fibres. Acta physiol. scand. **98**, 143—156 (1976)

FitzHugh, R.: A model of optimal voluntary muscular control. J. Math. Biol. **4**, 203—236 (1977)

Gibbs, C.L., Gibson, W.R.: Energy production of rat soleus muscle. Amer. J. Physiol. **223**, 864—871 (1972)

Grimby, L., Hannerz, J.: Firing rate and recruitment order of toe extensor motor units in different modes of voluntary contraction. J. Physiol. **264**, 865—879 (1977)

Hatze, H.: The complete optimization of a human motion. Math. Biosci. **28**, 99—135 (1976)

Hatze, H.: A myocybernetic control model of skeletal muscle. Biol. Cybernetics **25**, 103—119 (1977a)

Hatze, H.: The relative contribution of motor unit recruitment and rate coding to the production of static isometric muscle force. Biol. Cybernetics **27**, 21—25 (1977b)

Hatze, H.: A teleological explanation of Weber's law and the motor unit size law. CSIR Special Report WISK 248 (1977c)

Hatze, H., Buys, J.D.: Energy-optimal controls in the mammalian neuromuscular system. Biol. Cybernetics **27**, 9—20 (1977)

Henneman, E.: Peripheral mechanisms involved in the control of muscle. In: Medical Physiology, pp. 1697—1716. Mountcastle, V.B., ed. St. Louis: Mosby 1968

Henneman, E., Somjen, G., Carpenter, D.O.: Excitability and inhibitability of motoneurones of different sizes. J. Neurophysiol. **28**, 597—620 (1965)

Jewell, B.R., Wilkie, D.R.: The mechanical properties of relaxing muscle. J. Physiol. **152**, 30—47 (1960)

Jöbsis, F.F., O'Connor, M.J.: Calcium release and reabsorption in the sartorius muscle of the toad. Biochem. Biophys. Res. Commun. **25**, 246—252 (1966)

Julian, F.J.: The effect of calcium on the force-velocity relation of briefly glycerinated frog muscle fibres. J. Physiol. **218**, 117—145 (1971)

Kernell, D.: The limits of firing frequency in cat lumbosacral motoneurones possessing different time course of afterhyperpolarization. Acta physiol. scand. **65**, 87—100 (1965)

Milner-Brown, H.S., Stein, R.B., Yemm, R.: The orderly recruitment of human motor units during voluntary isometric contractions. J. Physiol. **230**, 359—370 (1973)

Person, R.S., Kudina, L.P.: Discharge frequency and discharge pattern of human motor units during voluntary contraction of muscle. Electroenceph. clin. Neurophysiol. **32**, 471—483 (1972)

Smit, G.L.: Biomechanical analysis of knee flexion and extension. J. Biomechanics **6**, 79—92 (1973)

Stark, L.: Neurological control systems, p. 311. New York: Plenum Press 1968

Thorstensson, A., Grimby, G., Karlsson, J.: Force-velocity relations and fiber composition in human knee extensor muscles. J. Appl. Physiol. **40**, 12—16 (1976)

Wendt, I.R., Gibbs, C.L.: Energy production of rat extensor digitorum longus muscle. Amer. J. Physiol. **224**, 1081—1086 (1973)

Received: October 11, 1977

Dr. H. Hatze
Nat. Res. Inst. for Math. Sciences
CSIR, B.O. Box 395
Pretoria 0001
South Africa